Research Square

Preprints are preliminary reports that have not undergone peer review.
They should not be considered conclusive, used to inform clinical practice,
or referenced by the media as validated information.

Machine Learning Identification of Static Plantar Pressure Features in Knee Osteoarthritis

He Xing
People's Hospital of Ningxia Hui Autonomous Region, Ningxia Medical University
Ma Tao
People's Hospital of Ningxia Hui Autonomous Region, Ningxia Medical University
Shang He
People's Hospital of Ningxia Hui Autonomous Region, Ningxia Medical University
Ma Biao
People's Hospital of Ningxia Hui Autonomous Region, Ningxia Medical University
Wang ruoyu
People's Hospital of Ningxia Hui Autonomous Region, Ningxia Medical University
Yang Tianxiang
People's Hospital of Ningxia Hui Autonomous Region, Ningxia Medical University
Li Jun
People's Hospital of Ningxia Hui Autonomous Region, Ningxia Medical University
Ding Yumei
People's Hospital of Ningxia Hui Autonomous Region, Ningxia Medical University
Chen Desheng
charles_cds@163.com

People's Hospital of Ningxia Hui Autonomous Region, Ningxia Medical University

Research Article

Keywords: Knee Osteoarthritis, Static Plantar Pressure, Machine Learning, Plantar Pressure Distribution, Biomechanics

Posted Date: June 3rd, 2026

DOI: https://doi.org/10.21203/rs.3.rs-9738661/v1

License: This work is licensed under a Creative Commons Attribution 4.0 International License.
Read Full License

Additional Declarations: No competing interests reported.

Machine Learning Identification of Static Plantar Pressure Features in Knee Osteoarthritis

He Xing[1];Ma Tao[1]; Shang He[1];Ma Biao[1];Wang ruoyu[1]Yang Tianxiang[1];Li Jun[1];Ding Yumei[1]; Chen Desheng[1*]

People's Hospital of Ningxia Hui Autonomous Region, Ningxia Medical University, Ningxia,Yinchuan, China,750000

Corresponding authors[1*]: Chen Desheng[1*] People's Hospital of Ningxia Hui Autonomous Region, Ningxia Medical University, Ningxia,Yinchuan, China,750000,Email：charles_cds@163.com

Abstract：Objective: This study aimed to characterize the static plantar pressure distribution patterns specific to unilateral knee osteoarthritis (KOA) and to develop a machine learning model based on plantar pressure asymmetry for KOA detection. The overarching goal was to establish an objective, non-invasive biomechanical framework to support early clinical assessment.**Methods:**This single-center, cross-sectional observational study enrolled 100 patients with unilateral KOA treated at the People's Hospital of Ningxia Hui Autonomous Region between January 2025 and March 2026. An equal number of age- and sex-matched healthy volunteers were recruited as controls. Static plantar pressure data were acquired using the eMat system. The foot was partitioned into ten anatomical regions, and the Asymmetry Index (AI) was calculated for each zone. Between-group comparisons of baseline characteristics and pressure metrics were performed using independent-samples*t*-tests and chi-square tests. The dataset was split into training and testing sets using a 7:3 stratified sampling ratio. Six machine learning algorithms were trained, and model performance was evaluated primarily by the area under the receiver operating characteristic curve (AUC). Model interpretability was assessed using SHAP (SHapley Additive exPlanations) values.**Results:**Patients with unilateral KOA exhibited a distinct pattern of static plantar pressure asymmetry. Specifically, the affected limb demonstrated a generalized reduction in overall load, with the most pronounced decreases observed in the medial heel and first metatarsal regions. Concurrently, a compensatory increase in loading was evident in the lateral metatarsal area. The Random Forest model, constructed using AI values from all ten anatomical zones, demonstrated superior predictive performance. On the independent test set, the model achieved an AUC of 0.997,

an accuracy of 95.0%, a sensitivity of 90.0%, and a specificity of 100%. Model interpretability analysis confirmed that an elevated heel region AI was the most influential biomechanical indicator for KOA identification, while the positive contribution of the lateral forefoot AI substantiated the presence of a lateral load compensation strategy.**Conclusion:**Unilateral KOA is associated with a quantifiable and characteristic pattern of static plantar pressure asymmetry. The Random Forest model developed using pressure asymmetry indices enables accurate identification of affected individuals. These findings offer a novel, objective approach for the early, non-invasive evaluation of KOA and provide a foundation for the development of personalized rehabilitation strategies.

Keywords: Knee Osteoarthritis; Static Plantar Pressure; Machine Learning; Plantar Pressure Distribution; Biomechanics

1 Background

1.1 Clinical Burden and Biomechanical Alterations in Knee Osteoarthritis

Knee osteoarthritis (KOA) is a highly prevalent degenerative joint disease characterized pathologically by articular cartilage degradation, subchondral bone sclerosis, and marginal osteophyte formation. The primary clinical manifestations include knee pain, stiffness, deformity, and restricted mobility, all of which markedly impair physical function and diminish quality of life[1]. Epidemiological data from China indicate that the prevalence of KOA among individuals aged 55 years and older reaches 13.2%, with a notably higher incidence in women than in men. The overall prevalence of symptomatic KOA is estimated at approximately 8.1%[2], and the disease burden continues to escalate in parallel with population aging[3].

Abnormal knee joint loading is a central biomechanical driver of KOA onset and progression. Under physiological conditions, the medial tibiofemoral compartment bears 60%–80% of the total load transmitted through the knee during the gait cycle and is therefore particularly susceptible to degenerative injury[4]. The chronic pain, quadriceps weakness, and impaired proprioceptive and neuromuscular control associated with KOA frequently precipitate deficits in postural balance. Given that the lower extremity functions as an integrated kinetic chain, biomechanical disturbances originating at the knee are transmitted distally along this chain, ultimately altering foot loading patterns[5]. Consequently, plantar pressure analysis constitutes a crucial tool for elucidating compensatory strategies and mechanisms of disease progression in individuals with KOA.

1.2 Current Applications of Plantar Pressure Analysis in KOA Research

Plantar pressure measurement provides a quantitative assessment of the magnitude and spatiotemporal distribution of ground reaction forces, enabling objective evaluation of lower limb biomechanical loading and postural stability. This technology is now widely applied across orthopedics, rehabilitation medicine, and sports science[6]. By segmenting the foot into discrete anatomical regions, clinicians and researchers can derive multidimensional parameters—including peak pressure, time to peak pressure, regional contact duration, and center of pressure trajectory—that collectively offer a quantitative framework for elucidating gait compensation strategies in individuals with KOA.

Previous investigations have documented characteristic alterations in plantar pressure parameters among patients with KOA, with the magnitude of these deviations correlating significantly with pain severity, physical function, and radiographic disease stage[7–9]. A common compensatory response involves a lateral shift in foot loading to reduce stress within the medial knee compartment, manifested as elevated lateral plantar pressures, altered pronation patterns, and diminished balance control[10, 11]. Additionally, studies have demonstrated that foot posture asymmetry is more pronounced in KOA patients than in healthy individuals and correlates positively with Kellgren–Lawrence grading[12, 13], underscoring the close association between interlimb loading asymmetry and disease progression.

Despite these advances, notable limitations persist in the current literature. First, research has predominantly focused on cross-sectional comparisons of dynamic plantar pressure between KOA patients and healthy controls[14], whereas investigations of static plantar pressure—particularly in early-stage KOA—remain sparse. Second, consensus is lacking regarding the quantitative relationship between KOA severity and plantar pressure distribution, as well as the differential asymmetry patterns exhibited in unilateral versus bilateral disease[15, 16]. Third, the clinical application of plantar pressure parameters in KOA management is hampered by an absence of standardized protocols. Conflicting findings concerning heel pressure alterations, for instance, may stem from confounding factors such as disease severity, walking speed, and concurrent foot deformities[17, 18]. Given that approximately 80% of individuals with unilateral KOA develop bilateral involvement within 12 years[19], characterizing plantar pressure profiles according to laterality and disease severity is imperative for informing early intervention and knee-preserving

treatment strategies.

1.3 Advantages of Machine Learning in Biomechanical Feature Identification

Machine learning algorithms are capable of automatically extracting salient features from high-dimensional datasets to enable accurate prediction and classification with minimal manual intervention[20], When integrated with wearable sensor technologies, these approaches have been successfully applied to biomechanical assessment across a spectrum of musculoskeletal conditions, including plantar fasciitis, fall risk evaluation, and post-stroke rehabilitation, demonstrating considerable translational potential[21, 22]. In the context of KOA research, investigators have developed machine learning models based on gait data for disease identification; however, existing studies exhibit notable limitations. The model reported by Wang et al[23] included only patients with end-stage KOA and healthy controls, thereby excluding individuals across varying disease severities and precluding analysis of biomechanical changes associated with disease progression.Other investigations have employed force platforms and three-dimensional motion capture systems to construct stratified KOA models[24], yet the prohibitive cost and technical complexity of such instrumentation restrict widespread implementation in primary care settings.

Static plantar pressure assessment offers distinct advantages, including portability, low cost, ease of operation, and independence from ambulatory performance.Coupling this modality with machine learning techniques circumvents the constraints inherent in conventional univariate statistical analyses, facilitating the extraction of core features from high-dimensional pressure data and the detection of subtle anomalies linked to KOA progression.This synergy provides a promising novel technical pathway for early KOA screening.

Against this backdrop, the present study was designed to achieve the following objectives: (1) to compare baseline demographic characteristics and static plantar pressure distribution patterns between patients with unilateral KOA and healthy controls; (2) to quantify bilateral plantar pressure differences in KOA patients using the Asymmetry Index (AI); and (3) to develop a machine learning model based on plantar pressure asymmetry patterns for automated KOA detection, with subsequent interpretation of key feature contributions, thereby furnishing an objective biomechanical foundation for gait assessment in KOA.

2 Methods

2.1 Study Population

This study employed a cross-sectional, observational design. A total of 100 patients with unilateral knee osteoarthritis (KOA) treated at the People's Hospital of Ningxia Hui Autonomous Region between January 2025 and March 2026 were enrolled. An equal number of matched healthy volunteers were concurrently recruited to serve as the control group.

2.2 Inclusion and Exclusion Criteria

Inclusion Criteria for the KOA Group:Participants were required to meet the following conditions: (1) a clinical diagnosis of unilateral symptomatic KOA according to the American College of Rheumatology (ACR) criteria, with radiographic evidence of Kellgren–Lawrence (K-L) grade ≥ II in the affected knee; (2) age between 45 and 75 years; (3) symptom duration of at least three months; (4) ability to stand independently and cooperate with static plantar pressure data acquisition; (5) no history of targeted KOA interventions—including pharmacotherapy, intra-articular injection, physical therapy, or structured rehabilitation—within the three months preceding enrollment; and (6) provision of written informed consent for voluntary study participation.

Exclusion Criteria for the KOA Group: Individuals were excluded if they presented with any of the following: (1) concomitant inflammatory arthropathies or structural knee disorders likely to impair lower limb function, such as rheumatoid arthritis, knee neoplasms, tuberculosis, or septic arthritis; (2) severe neurological, cardiovascular, cerebrovascular, or respiratory conditions, or other musculoskeletal disorders that could confound test results; (3) structural pathology or functional impairment of the spine, hip, or ankle–foot complex; (4) prior knee surgery or a history of lower limb trauma or surgical intervention resulting in structural foot deformity; (5) incomplete or technically inadequate static plantar pressure recordings; or (6) cognitive impairment precluding adherence to the testing protocol.

Inclusion Criteria for the Healthy Control Group: Eligibility required: (1) normal developmental history; (2) radiographic K-L grade 0 with no knee pain, swelling, or discomfort, and no prior diagnosis of KOA; (3) absence of lower limb surgical history or organic musculoskeletal disease; (4) ability to comply with static plantar pressure measurement

procedures; and (5) provision of written informed consent. The exclusion criteria applied to the control group were identical to those specified for the KOA group.

2.3 Ethical Approval

This study was conducted in strict accordance with the ethical principles for medical research involving human subjects outlined in the Declaration of Helsinki. The study protocol received approval from the Ethics Committee of the People's Hospital of Ningxia Hui Autonomous Region (Approval No. [2026]-YCKJ-013).All participants were fully informed of the study objectives, procedures, and potential risks, and each provided written informed consent prior to enrollment.

2.4 Baseline Data Collection

Demographic and baseline clinical characteristics were collected for all enrolled participants, including age, sex, height, body weight, and shoe size.

2.5 Static Plantar Pressure Measurement

Static plantar pressure data were acquired using a high-frequency pressure distribution measurement system (eMat Plantar Pressure Mapping System) with accompanying analysis software. All assessments were performed by a single, uniformly trained investigator. During measurement, participants were instructed to stand barefoot and stationary at the center of the pressure platform, with feet positioned naturally and gaze directed forward. Three repeated trials were conducted to ensure acquisition of at least three complete, valid recordings per foot (with the entire foot footprint falling within the active sensing area). The mean of the two most consistent trials was used for subsequent analysis. Using the software's automated ten-region segmentation algorithm (Figure 1), the plantar contact surface of each foot was divided into the following ten anatomical zones: medial heel, lateral heel, medial midfoot, lateral midfoot, first metatarsal, second metatarsal, lateral metatarsal, hallux, second toe, and lateral toes. The pressure-time integral (PTI) for each zone was calculated as the average pressure per unit area over the entire stance phase, and expressed as a percentage of the total plantar PTI (PTI%). This metric reflects the relative load distribution across discrete plantar regions during stance.

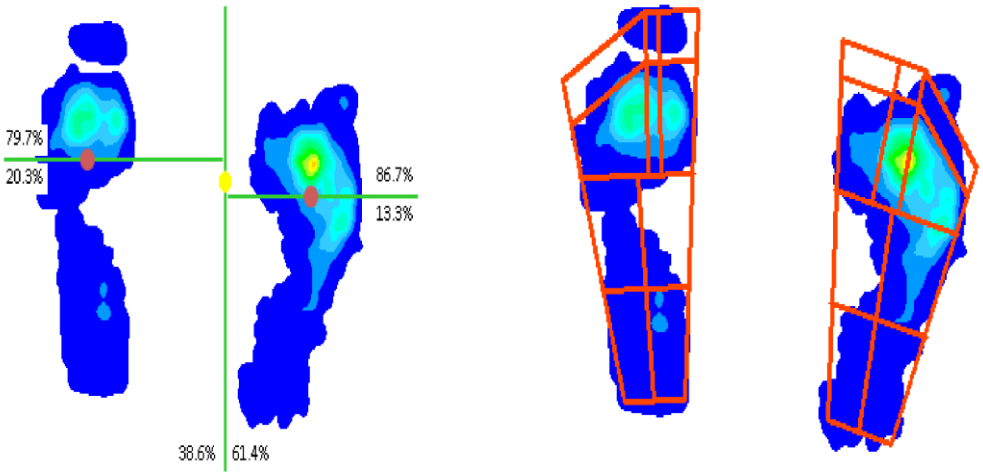


Figure 1: Static plantar pressure measurement and the ten-region foot segmentation scheme.

2.6 Statistical Analysis

Preliminary statistical analyses were performed using SPSS (version 26.0). Continuous variables were first assessed for normality using the Shapiro–Wilk test. Normally distributed data are presented as mean ± standard deviation ($\bar{x} \pm s$), and between-group comparisons were conducted using independent-samples *t*-tests. Non-normally distributed continuous variables are expressed as median with interquartile range [M (IQR)], and group differences were evaluated using the Mann–Whitney U test. Categorical variables are summarized as frequencies and percentages [n (%)], with comparisons performed using chi-square tests. A two-sided *p*-value < 0.05 was considered statistically significant.

Visualization of plantar pressure features was implemented using Python 3.9. Boxplots were generated for each anatomical region to illustrate distributional differences among the KOA affected limb, KOA unaffected limb, healthy left foot, and healthy right foot. Additionally, mean pressure heatmaps were constructed for the healthy control group (left vs. right foot) and the KOA group (affected vs. unaffected limb) to depict the spatial distribution patterns of bilateral plantar loading.

Machine Learning Model Development

The complete dataset (N = 200) was partitioned into a training set (70%, n = 140) and an independent test set (30%, n = 60) using stratified random sampling. For each of the ten anatomical regions, the Asymmetry Index (AI) was calculated as follows:

$$AI_i = \frac{| P_{\text{side1},i} - P_{\text{side2},i} |}{(P_{\text{side1},i} + P_{\text{side2},i})/2} \times 100\%$$

（For the KOA group, side 1 corresponds to the affected limb and side 2 to the unaffected limb; for the healthy control group, side 1 corresponds to the left foot and side 2 to the right foot.）

The ten AI values served as the input feature set for model training.Six machine learning algorithms were trained: Logistic Regression, Linear Support Vector Machine (SVM) with probability estimation enabled, Random Forest, XGBoost, LightGBM, and a Multi-Layer Perceptron (MLP) with a single hidden layer. Features were standardized using StandardScaler for distance-based models (Logistic Regression, Linear SVM, MLP), whereas the original AI values were retained for tree-based models (Random Forest, XGBoost, LightGBM). Hyperparameter optimization was performed on the training set using five-fold stratified cross-validation and grid search, with the area under the receiver operating characteristic curve (AUC) as the optimization metric. Each model was subsequently retrained on the full training set using the optimal hyperparameter configuration.

Model performance was evaluated on the independent test set using the following metrics: AUC (with 95% confidence interval), accuracy, sensitivity, specificity, and F1 score. Receiver operating characteristic (ROC) curves were plotted for all models. The model achieving the highest test-set AUC was designated as optimal, and its corresponding confusion matrix is reported. Feature importance for the optimal model was derived using built-in Gini importance. Global model interpretability was assessed by calculating SHAP (SHapley Additive exPlanations) values via TreeExplainer, and a SHAP summary plot was generated to illustrate the direction and magnitude of each feature's contribution.

3 Results

3.1 Participant Characteristics

A total of 100 patients with unilateral knee osteoarthritis (KOA) meeting the prespecified eligibility criteria were enrolled, alongside 100 randomly recruited healthy control subjects. Baseline demographic and anthropometric characteristics of the two groups are summarized in Table 1. Normality testing confirmed that all continuous variables followed a Gaussian distribution and are therefore presented as mean ± standard deviation ($\bar{x} \pm s$). Between-group comparisons revealed that the mean age of the KOA group (59.5 ± 7.4 years) was significantly

higher than that of the healthy control group (54.2 ± 10.9 years; *t* = 4.192, P < 0.001). No statistically significant differences were observed between the two groups with respect to sex distribution, body weight, height, or shoe size (all P > 0.05). With the exception of age, the core baseline characteristics of the two groups were well balanced, ensuring robust intergroup comparability.

Table 1: **Comparison of Baseline Characteristics between the KOA and Healthy Control Groups**

Variable	Healthy Control Group (n = 100)	KOA Group (n = 100)	*P*-value
Age (years)	54.2 ± 10.9	59.5 ± 7.4	<0.001†
Sex, n (%)	Female：51 (51.0%) Male：49（49.0%）	Female：54 (54.0%) Male：46（46.0%）	0.777
weight (kg)	64.6 ± 8.3	63.9 ± 8.3	0.485
Height (cm)	166.8 ± 7.4	168.7 ± 8.1	0.174
Shoe size (EU)	39.0 ± 2.5	39.1 ± 2.5	0.831

3.2 Comparison of Plantar Pressure Distribution

In the healthy control group, static plantar pressure exhibited a highly symmetric distribution between the left and right feet across all anatomical regions (Figure 2). The median values, interquartile ranges (IQR), and outlier distributions for the ten anatomical zones (A1–A10) were nearly identical, with no discernible systematic bias. Healthy individuals displayed a characteristic loading pattern wherein pressure magnitudes followed a descending gradient from the hindfoot to the forefoot and midfoot/toe regions. The highest pressure values were recorded in the medial (A1) and lateral (A2) heel zones, with median values ranging from 0.8% to 1.2% of body weight (%BW). Intermediate loading was observed in the first (A5) and second (A6) metatarsal regions, with median values approximating 0.6%–0.8% BW. The lowest pressures were documented in the medial/lateral midfoot (A3, A4) and all toe regions (A8–A10), with median values consistently below 0.3% BW. The proportion of outliers across all zones was negligible.

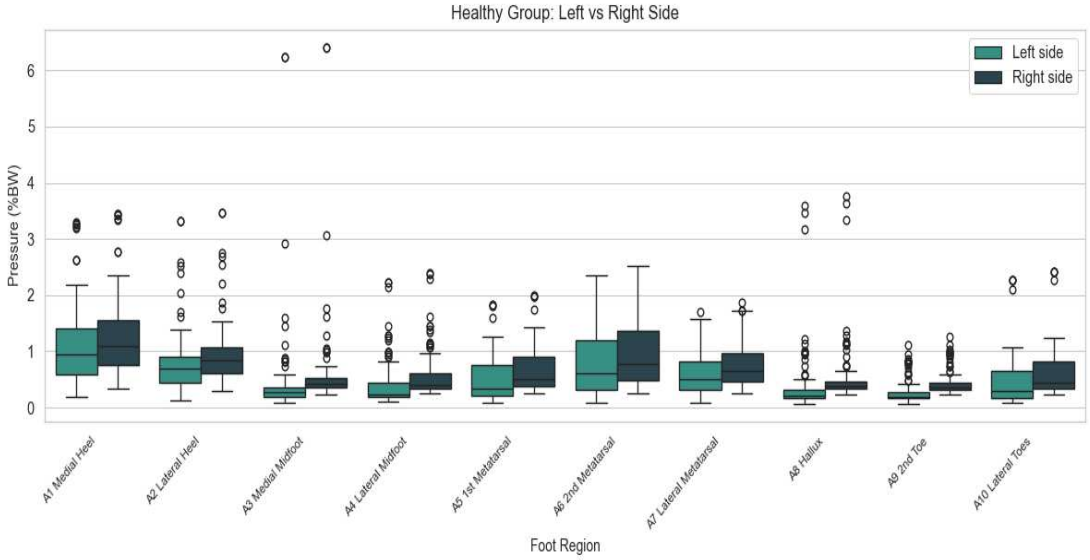


Figure 2: Boxplots comparing plantar pressure distribution between the left and right feet in the healthy control group across ten anatomical regions.

Boxplot analysis of the unilateral KOA group (Figure 3) revealed that median pressure values across all ten anatomical regions were consistently lower in the affected limb compared to the unaffected limb, indicating a generalized offloading pattern across the entire plantar surface. The most pronounced bilateral asymmetries were observed in the following regions: (1) Medial heel (A1): The median pressure in the affected limb was approximately 0.3% BW lower than that in the unaffected limb (affected: 0.5% BW vs. unaffected: 0.8% BW), with no overlap in interquartile ranges (IQR), signifying a substantial difference. (2) First metatarsal (A5): The affected limb exhibited a median reduction of 0.2%–0.3% BW relative to the unaffected limb, establishing this as a primary zone of forefoot offloading. (3) Lateral metatarsal (A7): The median pressure in the affected limb was marginally elevated by approximately 0.1% BW compared to the unaffected limb. Additionally, the IQR for most regions was wider in the affected limb than in the unaffected limb, suggesting greater inter-individual variability in static weight-bearing strategies among patients with KOA. Although absolute pressure values in the midfoot and toe regions were low, the affected limb nonetheless displayed lower values than the unaffected limb, further corroborating a generalized plantar offloading pattern.

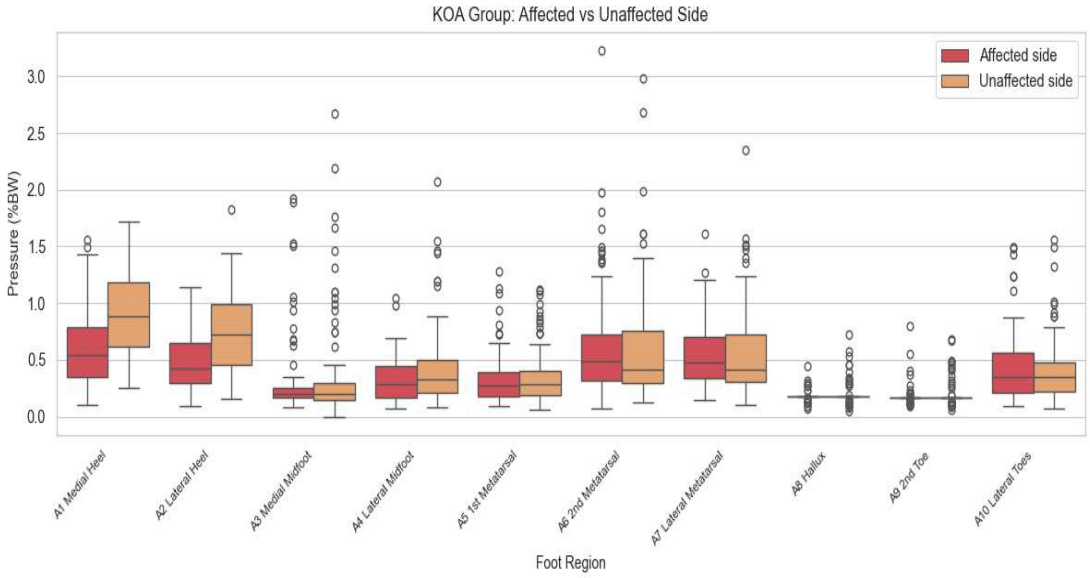


Figure 3: Boxplots comparing plantar pressure distribution between the affected and unaffected limbs in the unilateral KOA group across ten anatomical regions

In summary, the healthy control group exhibited a highly symmetric bilateral plantar pressure profile, characterized by elevated overall loading magnitude and minimal inter-individual variability. In contrast, the unilateral KOA group displayed marked bilateral pressure asymmetry, defined principally by a generalized reduction in loading across the entire affected plantar surface coupled with a compensatory load increase in the lateral metatarsal region. The anatomical zones exhibiting the most pronounced inter-group divergence were the medial heel (A1), first metatarsal (A5), and lateral metatarsal (A7) regions.

3.3 Mean Plantar Pressure Heatmap Analysis

In the healthy control group, the mean static pressure distribution exhibited a high degree of symmetry between the left and right feet, consistent with the loading pattern described in the preceding boxplot analysis (Figure 4). The heel (A1, A2) and metatarsal (A5–A7) regions constituted the primary weight-bearing zones with the highest recorded pressures, whereas the midfoot (A3, A4) and toe (A8–A10) regions demonstrated comparatively lower loading. Inter-foot pressure differences within corresponding anatomical zones were minimal. The largest absolute difference, observed in the hallux region (A8), was 0.16% BW (left: 0.40% BW vs. right: 0.56% BW); all other regional differences were below 0.15% BW, fluctuating within a narrow physiological range of 0.10%–0.15% BW. The heatmap visualization revealed a smooth, gradual color gradient transition bilaterally, devoid of focal abrupt changes, further confirming near-

perfect symmetry of static plantar pressure in healthy individuals.

In the unilateral KOA group, marked asymmetry in mean plantar pressure spatial distribution was evident between the affected and unaffected limbs (Figure 4). The key regions of disparity included: (1) Medial heel (A1): This was the most divergent zone, with mean pressure in the affected limb reduced by 0.31% BW relative to the unaffected limb, corresponding to a 34% decrease. (2) Midfoot (A3, A4): Mean pressure was notably lower in the affected limb. (3) First metatarsal (A5): Mean pressure in the affected limb decreased by 0.03% BW. (4) Lateral toes (A10): Mean pressure in the affected limb increased by 0.04% BW. (5) Second metatarsal (A6) and lateral metatarsal (A7): Mean pressure levels remained largely comparable between limbs.

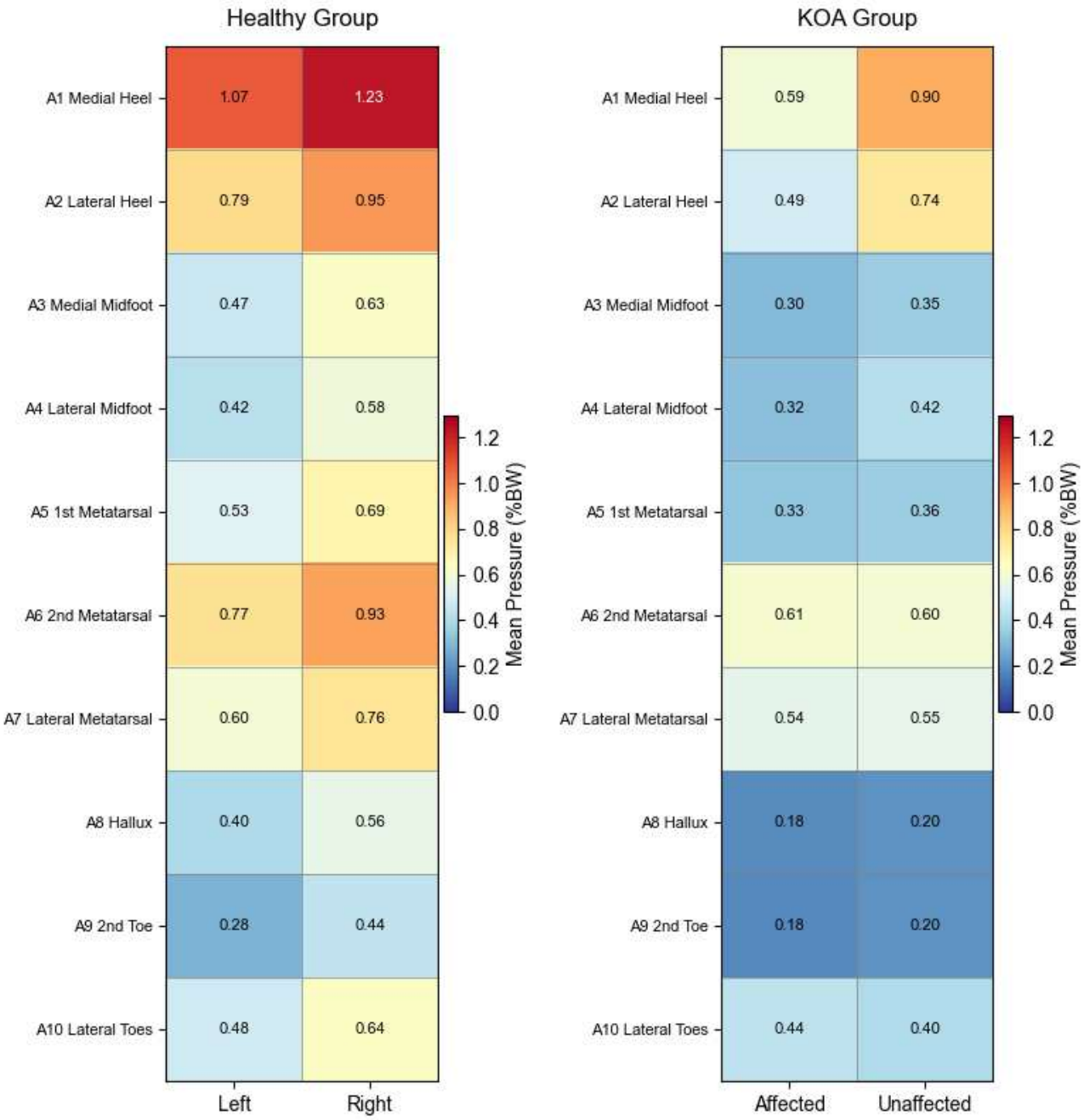


Figure 4: Mean plantar pressure heatmaps comparing the left and right feet in healthy controls and the affected versus unaffected limbs in the unilateral KOA group

3.4 Machine Learning Model Development and Performance Evaluation

A feature set was constructed using the Asymmetry Index (AI) values derived from the ten anatomical plantar regions. Six binary classification machine learning models were trained. Hyperparameter optimization for each algorithm was conducted via five-fold stratified cross-validation and grid search on the training set. Generalization performance was subsequently evaluated on an independent test set (n = 60). A comprehensive summary of model performance

metrics is presented in Table 2

Table 2: Performance Comparison of Machine Learning Models on the Independent Test Set

Model	AUC	Accuracy	Sensitivity	Specificity	F1 Score
Logistic Regression	0.896	0.767	0.700	0.833	0.750
Linear SVM	0.893	0.767	0.667	0.867	0.741
Random Forest	0.997	0.950	0.900	1.000	0.947
XGBoost	0.974	0.933	0.900	0.967	0.931
LightGBM	0.974	0.900	0.800	1.000	0.889
MLP	0.982	0.883	0.767	1.000	0.868

The Random Forest model demonstrated superior classification and discriminatory performance, achieving an area under the receiver operating characteristic curve (AUC) of 0.997 on the independent test set, along with an accuracy of 95.0%, sensitivity of 90.0%, specificity of 100%, and an F1 score of 0.947. The remaining tree-based models (XGBoost, LightGBM) and the multi-layer perceptron (MLP) also exhibited strong performance, with test-set AUC values exceeding 0.970. In contrast, logistic regression and linear support vector machine (SVM) yielded comparatively modest results, with AUC values ranging between 0.890 and 0.900. Visualization of the ROC curves (Figure 5) confirmed that the Random Forest model's curve was positioned closest to the upper-left corner relative to all competing models, substantiating its optimal discriminative capacity.

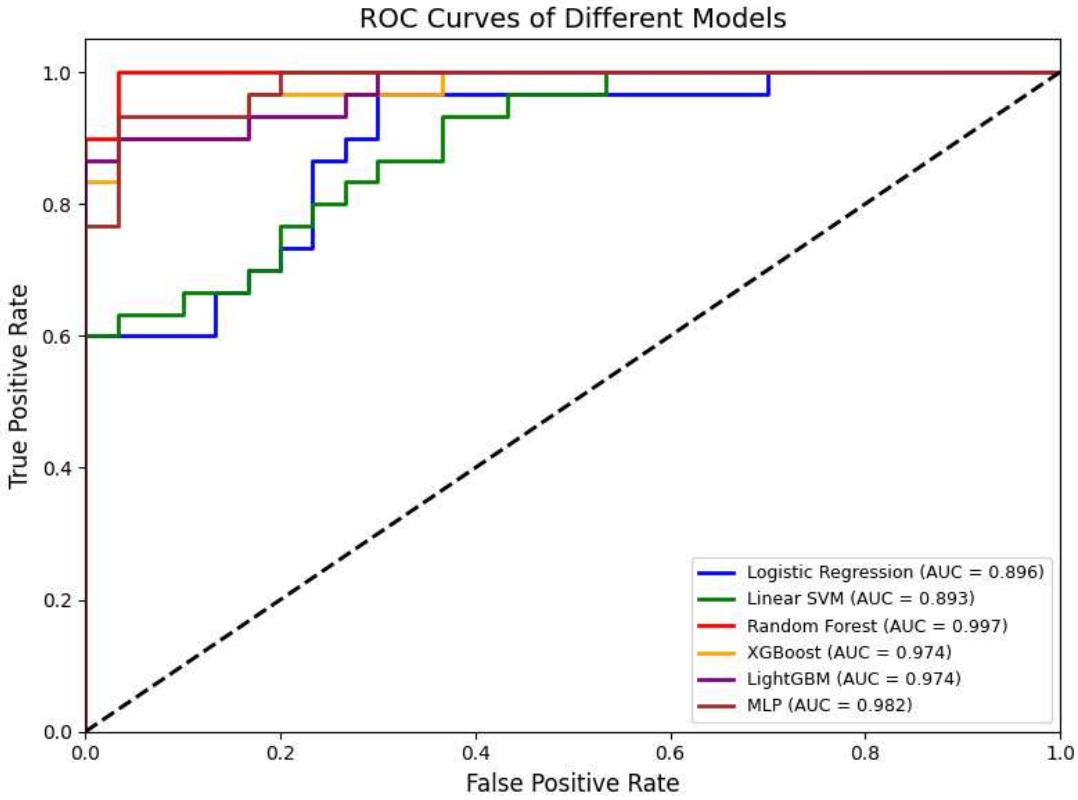


Figure 5: Receiver operating characteristic (ROC) curves for the six machine learning models evaluated on the independent test set

Analysis of the confusion matrix for the Random Forest model (Figure 6) revealed that all 30 healthy controls in the test set were correctly classified, yielding a specificity of 100%. Among the 30 patients with KOA, 27 were accurately identified, corresponding to a sensitivity of 90.0%. Only three KOA cases were misclassified as healthy controls. These findings collectively affirm the model's high discriminatory power and robust generalization capability.

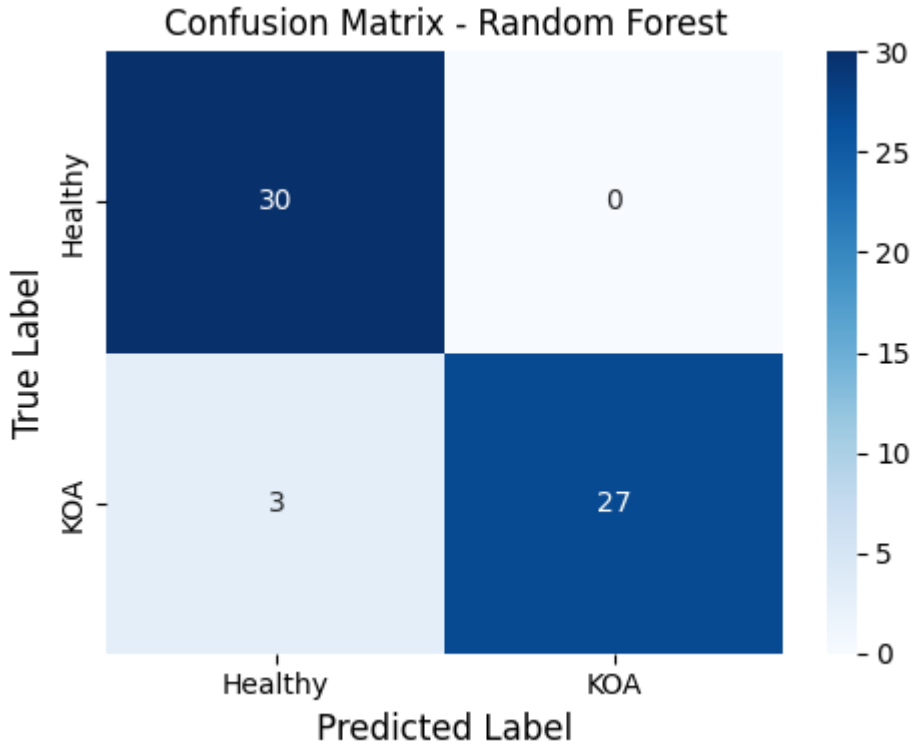


Figure 6: Confusion matrix illustrating the classification performance of the Random Forest model on the independent test set

Feature importance for the Random Forest model was assessed using built-in Gini impurity-based importance scores to quantify the contribution of each regional AI to the classification decision (Figure 7). The analysis revealed that the medial heel (A1) AI exhibited the highest feature importance (approximately 0.190), establishing it as the predominant determinant in model classification. This was followed by the second toe (A9; approximately 0.130) and hallux (A8; approximately 0.120) regions. The AI values for the medial midfoot (A3), lateral heel (A2), and lateral metatarsal (A7) regions also contributed meaningfully to the model's predictive capacity. In contrast, the first metatarsal (A5) AI demonstrated the lowest relative importance (approximately 0.020), suggesting that its independent contribution was limited and that it may exert influence through interactions with other features.

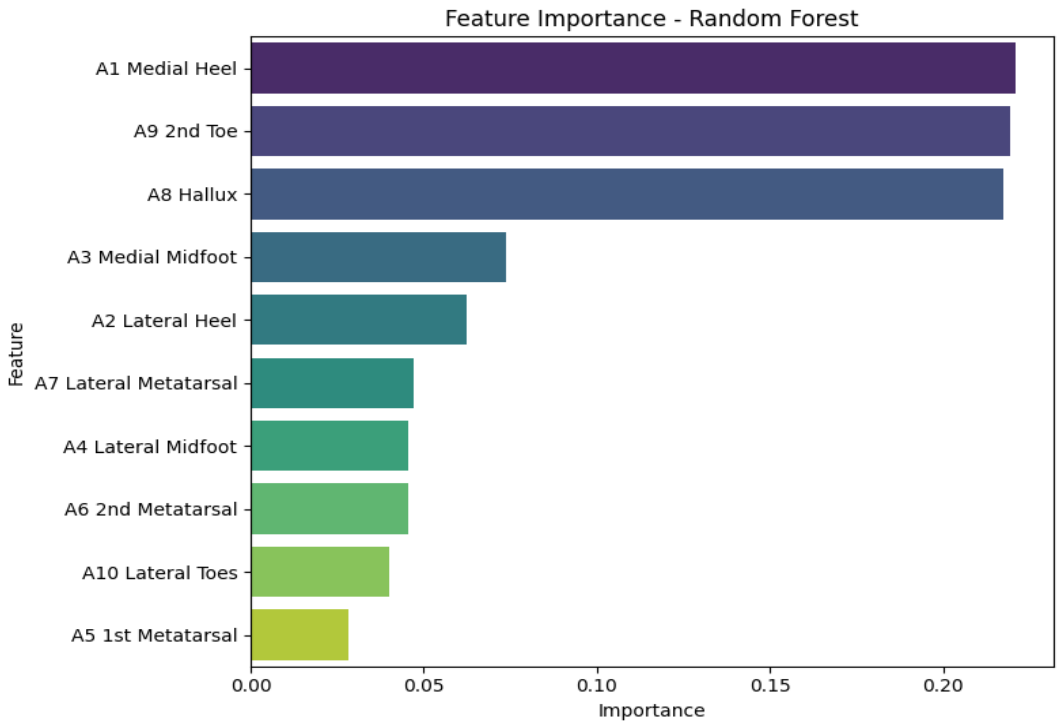


Figure 7: Feature importance ranking derived from the Random Forest model based on Gini impurity reduction

SHAP (SHapley Additive exPlanations) values for the Random Forest model were computed using TreeExplainer to elucidate the intrinsic decision-making mechanisms underlying model predictions (Figure 8). The analysis demonstrated a strong positive correlation between SHAP values and the AI of the medial heel (A1) and lateral heel (A2) regions (*r* > 0.84). This indicates that greater bilateral pressure asymmetry in the heel regions increased the likelihood of a KOA classification. Conversely, the AI values for the hallux (A8) and second toe (A9) regions exhibited a strong negative correlation with SHAP values (*r* < -0.84), suggesting that higher asymmetry in the toe regions was more strongly associated with a healthy classification. The AI values for the second metatarsal (A6), lateral metatarsal (A7), and lateral midfoot (A4) regions contributed positively to the model output, whereas the medial midfoot (A3) AI exhibited a weak negative contribution (*r* = -0.11).

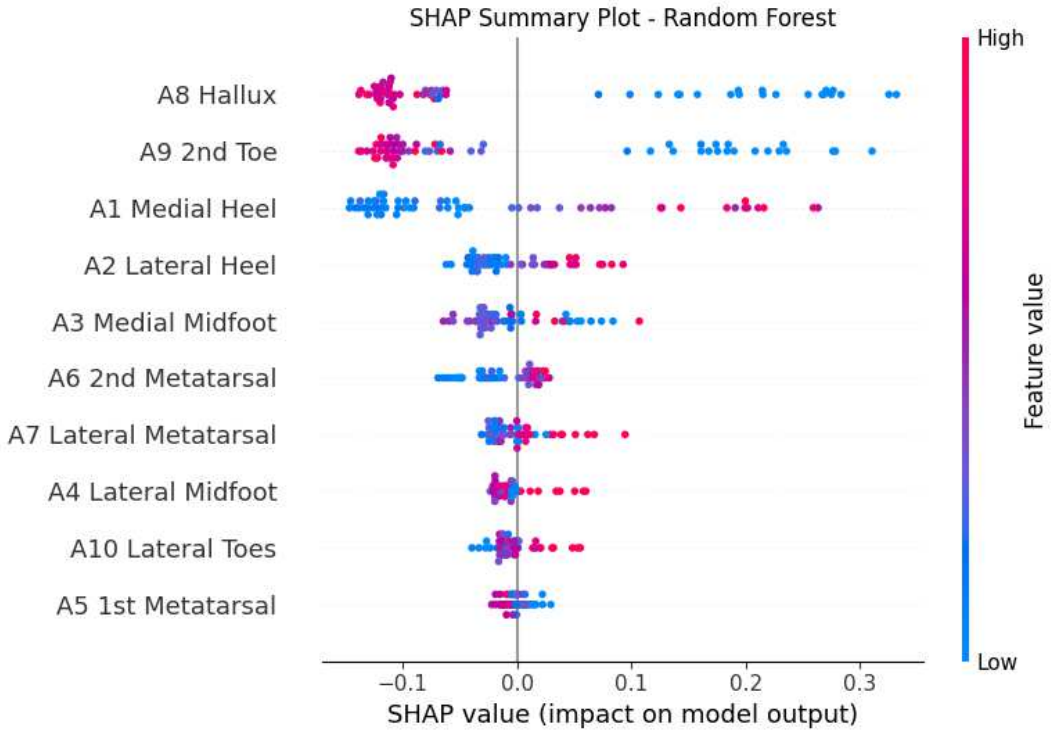


Figure 8: SHAP (SHapley Additive exPlanations) summary plot illustrating feature contributions to the Random Forest model predictions

In summary, interpretability analysis of the machine learning model confirmed that elevated asymmetry in the heel regions (A1, A2) constitutes the principal biomechanical hallmark for KOA identification. Mild asymmetry in the toe regions (A8, A9) was predominantly attributable to normal physiological variation. Furthermore, the positive contribution of the lateral forefoot regions substantiates the pain-avoidant, laterally shifted weight-bearing strategy characteristic of individuals with KOA.

4 Discussion

This study employed a ten-region foot segmentation approach to systematically characterize static plantar pressure distribution patterns in patients with unilateral knee osteoarthritis (KOA). The findings confirm that unilateral KOA is associated with a distinctive biomechanical profile characterized by a generalized reduction in loading across the entire plantar surface of the affected limb, marked bilateral pressure asymmetry, and a compensatory increase in loading within the lateral metatarsal region. Notably, bilateral pressure asymmetry in the medial heel and first metatarsal regions emerged as the core discriminative features distinguishing KOA patients from healthy controls. These results not only align with established biomechanical principles in KOA research but also address a critical gap in the literature by delineating static weight-bearing plantar pressure characteristics and asymmetry patterns specific to unilateral KOA. Collectively, this

evidence furnishes novel objective support for elucidating compensatory mechanisms operating throughout the lower extremity kinetic chain in individuals with KOA.

Under normal physiological conditions, the medial tibiofemoral compartment bears 60%–80% of the total load transmitted across the knee joint and consequently represents the primary site of involvement in KOA[4]. Previous investigations of plantar pressure in KOA have predominantly centered on dynamic gait scenarios, demonstrating that patients adopt a compensatory lateral shift in foot loading to reduce medial compartment stress, manifested as diminished medial forefoot loading and elevated lateral plantar pressures[25]. The present study extends these findings by confirming that this core biomechanical mechanism—characterized by pain-avoidant offloading and lateral compensation—is not exclusive to the dynamic gait cycle but also constitutes a defining feature of static weight-bearing in patients with unilateral KOA. Specifically, the median static pressure across all ten anatomical regions of the affected foot was lower than that of the unaffected foot, with the medial heel (A1) exhibiting a 34% reduction, thereby representing the predominant source of bilateral pressure asymmetry. This phenomenon is fundamentally attributable to active postural compensation: to circumvent stress concentration and nociceptive stimulation within the medial knee compartment, patients shift their center of mass toward the unaffected side via trunk lateral flexion and pelvic rotation, resulting in a generalized reduction in loading across the entire affected plantar surface. This interpretation aligns closely with prior reports of increased center of pressure sway amplitude and diminished postural control during static single-leg stance in individuals with KOA[26–29]. Moreover, the current study confirmed that healthy individuals exhibit a highly symmetric bilateral static plantar pressure distribution, with inter-foot pressure differences falling within normal physiological variation. This observation not only establishes a reliable physiological baseline for the construction of the Asymmetry Index (AI) but also corroborates that the bilateral pressure asymmetry evident in unilateral KOA constitutes a disease-related pathological alteration rather than a manifestation of normal physiological variance.

The present study further identified a significant reduction in pressure over the first metatarsal region (A5) of the affected limb, accompanied by a mild compensatory increase in the lateral metatarsal region (A7). These findings are consistent with those reported by Wang et al[30], who documented a progressive decline in the relative loading of the medial forefoot region on the affected side over the disease course. Prior research has largely attributed the diminished medial forefoot loading in KOA to restricted knee extension and insufficient propulsive force generation during the push-off phase of gait. Chronic pain and disuse atrophy of the quadriceps associated with KOA prolong the transition from knee flexion to extension during push-off and may preclude full terminal knee extension, ultimately compromising forefoot propulsion and reducing medial loading[31, 32]. However, the observation of pronounced medial forefoot offloading in the static weight-bearing context in the current study suggests that the underlying pathological mechanism extends beyond dynamic propulsive deficits and is intimately linked to lower limb alignment

compensation and neuromuscular protective inhibition during static stance. Chronic pain in KOA perpetuates quadriceps arthrogenic inhibition and strength deficits, concomitant with impairments in proprioception and neuromuscular control[31]. Consequently, patients actively avoid medial forefoot stress concentration even under static conditions, relying instead on compensatory loading of the lateral metatarsal region to maintain postural equilibrium. This finding substantiates the pan-contextual biomechanical evidence for the pain-avoidant, laterally shifted compensatory strategy in KOA. Furthermore, interpretability analysis of the machine learning model confirmed a positive contribution of lateral metatarsal AI to KOA classification, providing additional validation that lateral compensatory loading constitutes a characteristic biomechanical alteration in unilateral KOA.

Notably,the present study also identified a subtle lateral shift in plantar pressure distribution within the unaffected foot of patients with unilateral KOA, a finding consistent with prior reports[33]. The lower extremity functions as an integrated closed kinetic chain, wherein biomechanical disturbances originating at the knee are transmitted both proximally and distally along the chain[32]. The offloading and center-of-mass displacement toward the unaffected limb in unilateral KOA impose chronic supra-physiological loading on the contralateral lower extremity, thereby eliciting compensatory alterations in plantar pressure distribution. This persistent aberrant loading of the unaffected limb may not only precipitate secondary degenerative changes in the contralateral ankle and knee joints but also constitutes a critical pathological substrate underlying the progression from unilateral to bilateral disease. Indeed, previous studies indicate that approximately 80% of patients with unilateral KOA develop bilateral involvement within 12 years[19]. These findings underscore that clinical evaluation and intervention for unilateral KOA should extend beyond the affected knee to encompass compensatory biomechanical abnormalities in the contralateral limb. Early rehabilitative strategies aimed at correcting aberrant loading patterns in the unaffected limb may serve to attenuate disease progression and mitigate the risk of bilateral involvement.

Prior research on plantar pressure in KOA has largely concentrated on dynamic gait conditions, with relatively limited characterization of static plantar pressure profiles. Compared with dynamic gait analysis, static plantar pressure assessment offers distinct advantages, including ease of operation, low cost, excellent reproducibility, and independence from ambulatory performance. These attributes render it particularly well-suited for clinical evaluation of elderly, mobility-impaired, or severely symptomatic KOA patients. The present study systematically delineates the characteristic static plantar pressure distribution patterns in unilateral KOA and confirms that bilateral heel pressure asymmetry constitutes a core biomechanical marker for disease identification. These findings not only augment the theoretical framework for understanding lower limb compensatory mechanisms in KOA but also furnish an objective, clinically translatable biomechanical tool to support early screening, severity stratification, and the formulation of individualized rehabilitation protocols.

5 Conclusion

This study demonstrates that patients with unilateral knee osteoarthritis (KOA) exhibit a characteristic pattern of plantar pressure asymmetry during static weight-bearing, defined principally by a generalized reduction in loading across the entire affected plantar surface accompanied by a compensatory increase in lateral loading. The Random Forest model developed using plantar pressure asymmetry indices enables efficient and accurate identification of KOA, with heel region pressure asymmetry emerging as the core biomechanical marker distinguishing KOA patients from healthy individuals. The integration of static plantar pressure analysis with machine learning offers an objective biomechanical tool to support non-invasive assessment and rehabilitative intervention in KOA.

6 Limitations

Several limitations of this study warrant acknowledgment. First, the investigation employed a single-center, cross-sectional design with a sample of 200 participants recruited exclusively from the Ningxia region. The limited sample size and restricted geographic coverage constrain the generalizability of the findings, and the cross-sectional nature precludes inference of causal relationships between static plantar pressure characteristics and KOA. Second, the study cohort was restricted to patients with unilateral KOA, thereby excluding individuals with bilateral disease and those spanning the full disease continuum. The absence of longitudinal follow-up data further limits understanding of disease trajectory. Third, a statistically significant difference in baseline age between the two groups was observed, which may introduce minor residual confounding. Fourth, data collection was confined to static barefoot plantar pressure measurements, and the machine learning model underwent only internal validation. The study lacked integration of multi-dimensional biomechanical parameters and external independent validation.

7 Declarations

7.1 Ethics approval and consent to participate

This study was approved by the Ethics Committee of the People's Hospital of Ningxia Hui Autonomous Region (Approval No. [2026]-YCKJ-013). Written informed consent was obtained from all individual participants included in the study.

7.2 Consent for publication

Not applicable. This study does not contain any identifiable images or personal/clinical

details of the participants.

7.3 Open access

By submitting this article, I agree to pay the article processing charge (APC) in full if the manuscript is accepted for publication, unless the charge is covered by an institutional agreement or journal partner, or a full waiver has been granted.

7.4 Competing interests

I declare that the authors have no competing interests as defined by BMC, or other interests that might be perceived to influence the results and/or discussion reported in this paper.

7.5 Dual publication

The results/data/figures in this manuscript have not been published elsewhere, nor are they under consideration (from me or any of the contributing authors) by another publisher.

7.6 Authorship

I confirm that the corresponding author has read the journal policies and submits this manuscript in accordance with those policies.

7.7 Third party materia

All of the material is owned by the authors and/or no permissions are required.

7.8 Data availability

The datasets used and/or analyzed during the current study are available from the corresponding author on reasonable request. All data supporting the conclusions of this article are included in the manuscript and its supplementary files. The statistical code used in this study is available from the corresponding author upon reasonable request for non-commercial purposes.

Clinical trial number: Not applicable.

8 References

[1] BOUCHOURAS G, SOFIANIDIS G, PATSIKA G, et al. Women with knee osteoarthritis increase knee muscle co-contraction to perform stand to sit [J]. Aging Clin Exp Res, 2020, 32(4): 655-62.

[2] HUNTER D J, BIERMA-ZEINSTRA S. Osteoarthritis [J]. Lancet, 2019, 393(10182): 1745-59.

[3] LAWFORD B J, BENNELL K L, HABER T, et al. Osteoarthritis Year In Review 2024: Rehabilitation and outcomes [J]. Osteoarthritis Cartilage, 2024, 32(11): 1405-12.

[4] KHAN S J, KHAN S S, USMAN J, et al. Combined effects of knee brace, laterally wedged insoles, and toe-out gait on knee adduction moment and fall risk in moderate medial knee osteoarthritis patients [J]. Prosthet Orthot Int, 2019, 43(2): 148-57.

[5] SAZO-RODRíGUEZ S, MéNDEZ-REBOLLEDO G, GUZMáN-MUñOZ E, et al. The effects of progressive neuromuscular training on postural balance and functionality in elderly patients with knee osteoarthritis: a pilot study [J]. J Phys Ther Sci, 2017, 29(7): 1229-35.

[6] Li SH, Li Q, Li Z, et al. Plantar pressure and gait analysis in patients with anterior cruciate ligament injury and after reconstruction surgery [J]. Chinese Journal of Tissue Engineering Research, 2023, 27(04): 626–631.

[7] Wang LC, Chen H, Zhang HL, et al. A study on the temporal distribution patterns of dynamic plantar loading in bilateral knee osteoarthritis [J]. Chinese Journal of Rehabilitation Medicine, 2020, 35(08): 944–948.

[8] RøSLAND T, GREGERSEN L S, ESKEHAVE T N, et al. Pain sensitization and degenerative

changes are associated with aberrant plantar loading in patients with painful knee osteoarthritis [J]. Scand J Rheumatol, 2015, 44(1): 61-9.

[9] ZHANG Z, WANG L, HU K, et al. Characteristics of Plantar Loads During Walking in Patients with Knee Osteoarthritis [J]. Med Sci Monit, 2017, 23: 5714-9.

[10] FRYZOWICZ A, MURAWA M, KABACIŃSKI J, et al. Reference values of spatiotemporal parameters, joint angles, ground reaction forces, and plantar pressure distribution during normal gait in young women [J]. Acta Bioeng Biomech, 2018, 20(1): 49-57.

[11] LIDTKE R H, MUEHLEMAN C, KWASNY M, et al. Foot center of pressure and medial knee osteoarthritis [J]. J Am Podiatr Med Assoc, 2010, 100(3): 178-84.

[12] CHEN Z, SHEN Z, YE X, et al. Association between Foot Posture Asymmetry and Static Stability in Patients with Knee Osteoarthritis: A Case-Control Study [J]. Biomed Res Int, 2020, 2020: 1890917.

[13] CHEN Z, YE X, SHEN Z, et al. Comparison of the Asymmetries in Foot Posture and Properties of Gastrocnemius Muscle and Achilles Tendon Between Patients With Unilateral and Bilateral Knee Osteoarthritis [J]. Front Bioeng Biotechnol, 2021, 9: 636571.

[14] GILADI N, HERMAN T, REIDER G, II, et al. Clinical characteristics of elderly patients with a cautious gait of unknown origin [J]. J Neurol, 2005, 252(3): 300-6.

[15] CREABY M W, BENNELL K L, HUNT M A. Gait differs between unilateral and bilateral knee osteoarthritis [J]. Arch Phys Med Rehabil, 2012, 93(5): 822-7.

[16] MARMON A R, ZENI J A, JR., SNYDER-MACKLER L. Perception and presentation of function in patients with unilateral versus bilateral knee osteoarthritis [J]. Arthritis Care Res (Hoboken), 2013, 65(3): 406-13.

[17] ELBAZ A, MOR A, SEGAL G, et al. Novel classification of knee osteoarthritis severity based on spatiotemporal gait analysis [J]. Osteoarthritis Cartilage, 2014, 22(3): 457-63.

[18] HE Y J, ZHENG X L, WANG D F, et al. Static and Dynamic Plantar Pressure Distribution in 94 Patients with Different Stages of Unilateral Knee Osteoarthritis Using the Footscan® Platform System: An Observational Study [J]. Med Sci Monit, 2023, 29: e938485.

[19] METCALFE A J, ANDERSSON M L, GOODFELLOW R, et al. Is knee osteoarthritis a symmetrical disease? Analysis of a 12 year prospective cohort study [J]. BMC Musculoskelet Disord, 2012, 13: 153.

[20] GIAMBAGLI L, BUFFONI L, CARLETTI T, et al. Machine learning in spectral domain [J]. Nat Commun, 2021, 12(1): 1330.

[21] CHEN X, HU D, ZHANG R, et al. Interpretable evaluation for the Brunnstrom recovery stage of the lower limb based on wearable sensors [J]. Front Neuroinform, 2022, 16: 1006494.

[22] MERRY K J, MACDONALD E, MACPHERSON M, et al. Classifying sitting, standing, and walking using plantar force data [J]. Med Biol Eng Comput, 2021, 59(1): 257-70.

[23] WANG A, LI D, FAN N, et al. Piezoresistive-Based Gait Monitoring Technique for the Recognition of Knee Osteoarthritis Patients [J]. IEEE Access, 2022, 10: 123874-84.

[24] KWON S B, KU Y, HAN H S, et al. A machine learning-based diagnostic model associated with knee osteoarthritis severity [J]. Sci Rep, 2020, 10(1): 15743.

[25] AKIMOTO T, KAWAMURA K, WADA T, et al. Gait cycle time variability in patients with knee osteoarthritis and its possible associating factors [J]. J Phys Ther Sci, 2022, 34(2): 140-5.

[26] Peng WJ, Luo X, Zhang D, et al. Efficacy of proprioceptive training in the treatment of knee osteoarthritis and its effects on gait characteristics and balance function [J]. Journal of Clinical

and Experimental Medicine, 2020, 19(01): 102–105.

[27] AL-ZAHRANI K S, BAKHEIT A M. A study of the gait characteristics of patients with chronic osteoarthritis of the knee [J]. Disabil Rehabil, 2002, 24(5): 275-80.

[28] KAUFMAN K R, HUGHES C, MORREY B F, et al. Gait characteristics of patients with knee osteoarthritis [J]. J Biomech, 2001, 34(7): 907-15.

[29] ORNETTI P, MAILLEFERT J F, LAROCHE D, et al. Gait analysis as a quantifiable outcome measure in hip or knee osteoarthritis: a systematic review [J]. Joint Bone Spine, 2010, 77(5): 421-5.

[30] Wang X, Luo W, Huang WZ, et al. Correlation between clinical staging of unilateral knee osteoarthritis and bilateral plantar pressure [J]. Chinese Journal of Tissue Engineering Research, 2021, 25(27): 4312–4317.

[31] Le Y, Jin RJ, Yang Y, et al. Analysis of knee osteoarthritis from the perspective of lower limb biomechanics [J]. Chinese Journal of Rehabilitation Theory and Practice, 2013, 19(06): 505–509.

[32] SAITO I, OKADA K, WAKASA M, et al. Foot pressure pattern, hindfoot deformities, and their associations with foot pain in individuals with advanced medial knee osteoarthritis [J]. Gait Posture, 2018, 59: 83-8.

[33] DEMIK D E, MARINIER M C, GULBRANDSEN T R, et al. Does Isolated Unilateral Hip or Knee Osteoarthritis Lead to Adverse Changes in Extremity Composition? [J]. Iowa Orthop J, 2022, 42(1): 163-7.